Hardrock 3D Seismic Imaging of the Mawson Prospect

Jie Jian Leong
Terra Resources
j.leong@terraresources.com.au

Barry Bourne
Terra Resources
b.bourne@terraresources.com.au

SUMMARY

The Mawson prospect is home to a massive nickel-copper sulphide discovery that sits within the Fraser Range District of the Albany-Fraser Orogen in Western Australia that also contains the Nova-Bollinger and Silver Knight Deposits. Since its initial discovery, the exploration program has been expanded to include a 3D seismic survey to define the Mawson intrusion architecture. Seismic imaging was performed in pre-stack time migration (PSTM) and pre-stack depth migration (PSDM), and petrophysical measurements including P-wave velocity and density obtained from drill core samples were utilised to build the confidence of seismic velocity model. Several wireline geophysical loggings that have been conducted recently show a strong correlation with key seismic reflectors associated with the chonolith. The resulting seismic cube has enabled the chonolith to be mapped below the Mawson Fault, which supports the theory that the intrusion continues at depth below the existing drilling program.

INTRODUCTION

The Mawson prospect is home to a massive nickel-copper sulphide discovery that sits within the Fraser Range District of the Albany-Fraser Orogen in Western Australia that also contains the Nova Bollinger and Silver Knight Deposits. The project started in 2015 when host rocks were identified based on having similar, unique magnetic signature as the Nova-Bollinger deposit and high-density anomaly on gravity. Subsequent exploration programs including drilling and various geophysical applications have provided success in discovering massive nickel-copper (Ni-Cu) sulphide mineralisation. However, the direct detection of these mineralisation has always been challenging due to conductive stratigraphic covers and graphitic units that are masking the zone of mineralisation. As a result, a 3D seismic program was conducted to provide new information on structural and stratigraphic architecture of the Mawson prospect.

LOCAL GEOLOGY

The Albany–Fraser Orogen is a Proterozoic orogenic belt that lies along the southern and southeastern margin of the Archean Yilgarn Craton. The orogen is divided into two tectonic components: the dominantly Archean Northern Foreland and the dominantly Proterozoic Kepa Kurl Booya Province (Spaggiari et al., 2014). This province is further subdivided into the dominantly Paleoproterozoic Biranup and Nornalup Zones, and the Mesoproterozoic Fraser Zone. The Fraser Zone is bounded by Fraser Shear Zone to the west and Boonderoo Shear Zone to the east and hosts the Mawson massive nickel sulphide mineralisation.

EARLY CHALLENGES

One of the early challenges is that both electromagnetic and induced polarisation response were affected by close proximity of strongly conductive transported covers and graphitic units within the metasedimentary package. High-powered electromagnetic transmitter and superconducting quantum interfering device (SQUID) were used but it was still challenging to detect Ni-Cu sulphide mineralisation in the presence of these stratigraphic conductors.

3D SEISMIC

The seismic survey was based on a hybrid design with variable sources and receivers' line and station spacing, whereby densely-spaced receivers were placed around known shallower mineralisation corridor in the west and the sources' location were based on utilising existing tracks and drill access. Similar hardrock 3D seismic case studies including Kevitsa survey in Finland and Kambalda survey in Western Australia were used as a reference for seismic waveform modelling and parameterisation.

Core-measured density and P-wave velocity from 2 drillholes were used to generate the initial velocity model for seismic processing. Pre-stack depth migration was performed and a few angular mutes were generated for the seismic stacks.

The resulting interpretation has clearly imaged the Mawson Fault, a prominent event that is prevalent throughout the entire seismic cube. The resulting drillhole reconciliation with seismic has established that the chonolith extends below the Mawson Fault. Generation of seismic cube at different angle mutes has also enhanced the imaging of ultramafic and chonolith lithologies within the first 250 m section of the seismic cube.

PETROPHYSICS

A full suite of wireline petrophysical data was acquired on 5 drillholes, including gamma, density, velocities, magnetic susceptibility and resistivity. Figure 1(a) illustrates the comparison between wireline P-wave velocity, core-measured P-wave velocity, and PSDM velocity. The petrophysical data has provided an increased confidence in velocity measurement to provide better velocity model for future seismic re-processing and inversion.

DISCUSSIONS

Given the relative cost of acquiring 3D seismic which is normally expensive, the cost efficiency of seismic acquisition and processing was able to be maintained. One of them is that existing tracks and drill access were utilised by vibroseis for sources' placement. Staggering crew management was also arranged to allow crew accommodation on site at a comfortable capacity. Lastly, new petrophysical data and historical case studies were utilised to provide better scenarios and parameterisation for both seismic acquisition and processing.

Petrophysical analysis has shown that it can differentiate between ultramafic and mafic rocks, but more measurement is required. As illustrated in Figures 1(b) and 1(c), ultramafic and mafic rocks can be identified in seismic but the density range of this measurement is only up to 2.95 g/cc. Another acoustic impedance plot over the entire Fraser Range as illustrated in Figure 2 shows that the mineralisation from the Nova-Bollinger deposit has a very high density of 4.5 g/cc. This shows that given that each iso-contour represents an acoustic impedance contrast, it is not possible to discern the mineralisation against these other rock types that lies on the same iso-contour line.

Seismic interpretation has also shown that there could be structural implication in place when interpreting chonolith below the Mawson Fault. As illustrated in Figure 3, a reverse fault could be present based on the following observations: (a) fault-propagation fold above the reverse fault; (b) similar fault offset between the Mawson Fault and chonolith horizons; (c) strong correlation with a steeping conductor identified from fixed-loop electromagnetic (FLEM) survey; (d) flattening of Mawson Fault horizon showed similar attributes between the Mawson Fault horizon itself; and (e) downward-plunging gravity inversion shell coincides with fault contact zone (Figure 3(d)).

CURRENT CHALLENGES

At this stage, the mineralisation could not be identified directly. Steeping structures that were recognised in drill cores could not be imaged with the current seismic imaging, which requires a more expensive migration algorithm including reverse time migration (RTM) and least-squares Kirchhoff migration (LSMIG) to image such structures.

CONCLUSIONS

3D seismic has enabled the chonolith to be mapped below the Mawson Fault. There is a strong theory that the intrusion continues at depth below the existing drilling program. Mineralisation could not be detected with the current seismic imaging but re-processing with advanced knowledge and technology could be able to unearth it. More studies are needed to be done on seismic and petrophysical interpretation to establish structural and stratigraphic architecture.

ACKNOWLEDGMENTS

We would like to acknowledge Legend Mining for giving us the permission to publish this paper. We would also like to acknowledge HiSeis, Terra Petrophysics, Mustagh Resources and Geological Survey of Western Australia for their contribution to this work. Last but not least, we would like to thank dGB Earth Sciences and REFLEX for their software contribution.

REFERENCES

Brisbout, L.I., 2015, Determining crustal architecture in the east Albany–Fraser Orogen from geological and geophysical data: Geological Survey of Western Australia, Report 152, 52p.

Kirkland, C.L., Evans, K.A., Hartnady, M.I.H., Walker, A.T., Chard, J., Clark, C., Spaggiari, C.V., Quentin de Gromard, R., Reddy, S., Smithies, R.H., Kiddie, O.C. and Barham, M., 2020, MRIWA M0470 final report — Mineral systems on the margins of cratons: Albany–Fraser Orogen / Eucla basement case study, an executive summary: Geological Survey of Western Australia, Record 2020/5, 23p.

Mortimore, C., Trunfull, J. and Bourne, B., 2022, Regional petrophysics: Albany-Fraser Orogen 2021–22: Geological Survey of Western Australia, Report No. 72201, 28p.

Spaggiari, C.V., Kirkland, C., Smithies, R.,Occhipinti, S. and Wingate, M., 2014, Geological framework of the Albany-Fraser Orogen.
Spaggiari, C.V. and Tyler, I.M., 2014, Albany–Fraser Orogen seismic and magnetotelluric (MT) workshop 2014: extended abstracts: Geological Survey of Western Australia, Record 2014/6, 182p.

Spaggiari, C.V., Occhipinti, S.A., Korsch, R.J., Doublier, M.P., Clark, D.J., Dentith, M.C., Gessner, K., Doyle, M.G., Tyler, I.M., Kennett, B.L.N., Costelloe, R.D., Fomin, T. and Holzschuh, J., 2014b, Interpretation of Albany–Fraser seismic lines 12GA-AF1, 12GA-AF2 and 12GAAF3: implications for crustal architecture, in Albany–Fraser Orogen seismic and magnetotelluric (MT) workshop 2014: extended abstracts compiled by C.V. Spaggiari and I.M. Tyler: Geological Survey of Western Australia, Record 2014/6, p. 28–43.

Spaggiari, C.V. and Pawley, M.J., 2012, Interpreted pre-Mesozoic bedrock geology of the east Albany-Fraser Orogen and southeast Yilgarn Craton (1:500 000), in The geology of the east Albany-Fraser Orogen - a field guide compiled by C.V. Spaggiari, C.L. Kirkland, M.J. Pawley, R.H. Smithies, M.T.D. Wingate, M.G. Doyle, T.G. Blenkinsop, C. Clark, C.W. Oorschot, L.J. Fox, and J. Savage: Geological Survey of Western Australia, Record 2011/23, Plate 1A.

Figures

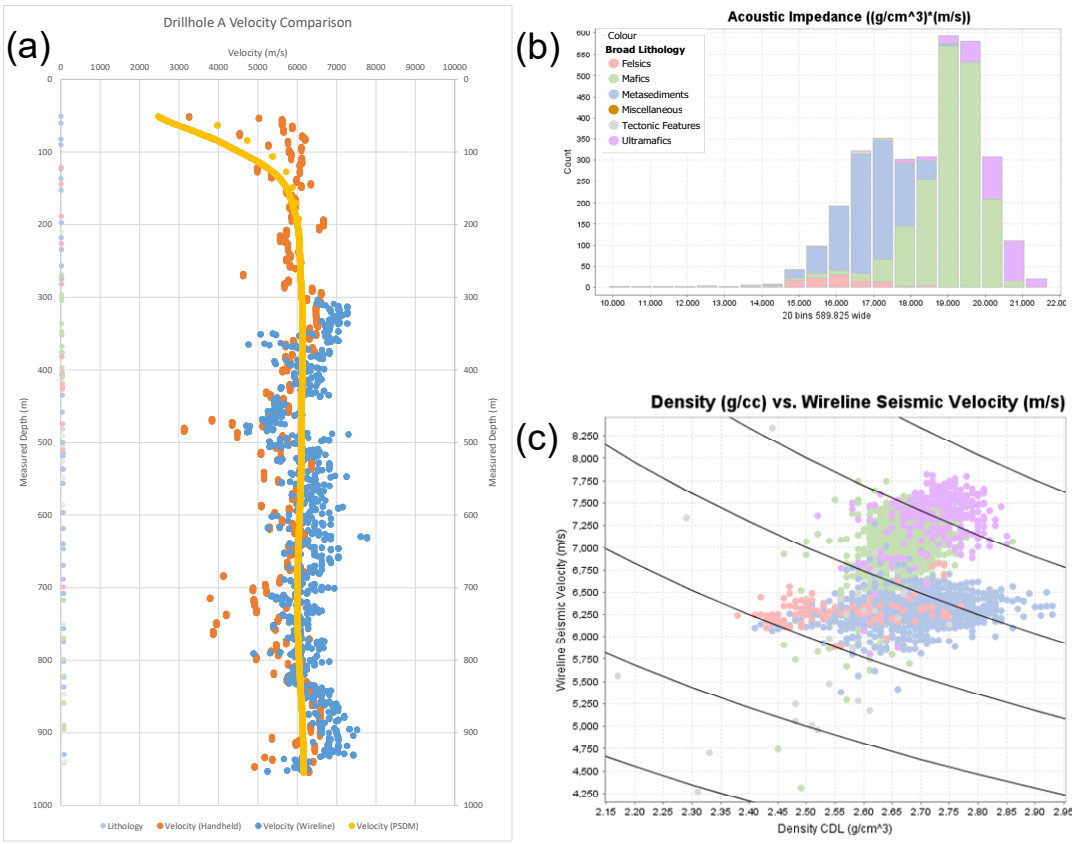

Figure 1. Petrophysical results from drillhole A. (a) Velocities comparison between wireline (blue), core-measured P-wave (orange) and PSDM velocities (yellow); (b) histogram distribution of acoustic impedance for each lithology; and (c) wireline P-wave velocity versus density plot with constant acoustic impedance iso-contours at 0.06 reflection coefficient.

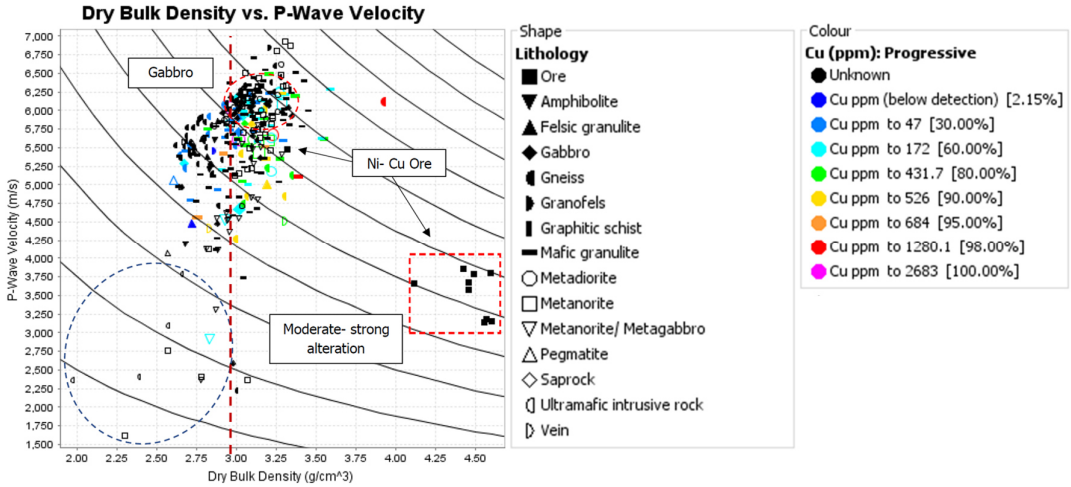

Figure 2. Core-measured P-wave velocity versus density plot with constant acoustic impedance iso-contours at 0.06 reflection coefficient obtained from GSWA-Terra Petrophysics Report No. 72201, showing massive sulphides response from Nova-Bollinger deposit (in red-dashed rectangle). Note that the measured density range from drillhole A (Figure 1) is only up to 2.95 g/cc (red-dashed line).

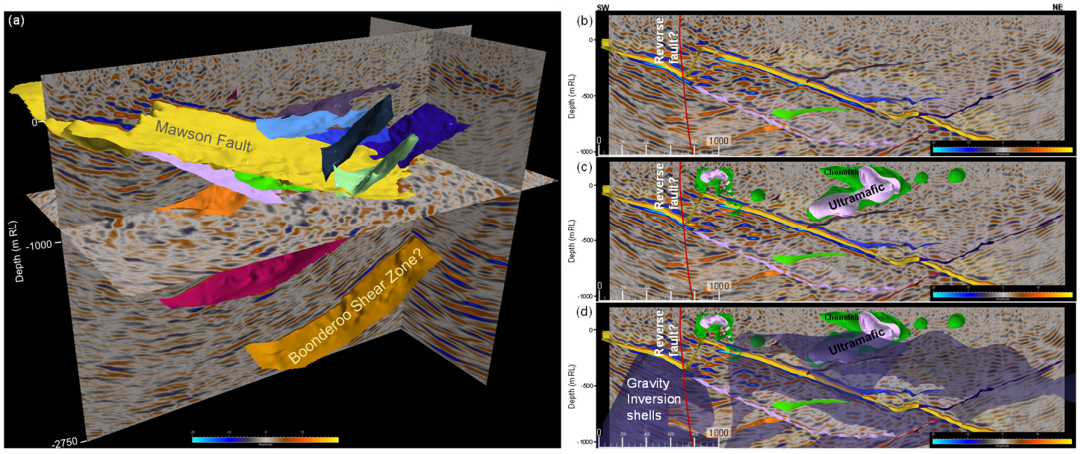

Figure 3. (a) A 3D perspective of PSDM cube; (b) seismic interpretation; (c) with geological wireframes of chonolith and ultramafic; and (d) gravity inversion shell.